

AUTOMATIC EXTRACTION OF LANDCOVER THEMES ON DIGITAL ORTHOPHOTOS IN MOUNTAINOUS AREA FOR MAPPING AT 1/25K

H. Le Men, J. Trévisan, D. Boldo

Institut Géographique National, direction technique, 2 av. Pasteur 94165 Saint-Mandé Cedex France

Commission II, WG II/4

KEY WORDS: Radiometric corrections- data fusion- uncertainty management- landcover-knowledge based interpretation

ABSTRACT:

IGN-F is undertaking the production of a new digital 1/25k national base map. In this context, we developed an automatic process for extracting landcover information out of digital orthophotos. This process must be robust, self-adaptive for variation of image quality, date of acquisition, geographical location..., and must be usable also in an updating context. For this, we used a general strategy of information fusion from different sources: DTM, general geographic a priori knowledge, old or imprecise information. The uncertainty is managed throughout the full process until the final cartographic representation.

More precisely, the images are first corrected for atmospheric effects, shadows, sun exposition... Probability functions for the different themes, knowing image radiometry, altitude, slope, orientation, are built. All these informations are merged using a simple form of Dempster Shafer rule on pixel basis. The pixel information is then extended to regions obtained by an image segmentation.

1. GENERAL CONTEXT

The French national surveying and mapping agency (IGN-F) is carrying out a national topographic database. The data capture began in 1989 and will be finished in 2006. A new version of the basic map at scale 1/25k should progressively be done with a full digital process out of this database, but for different reasons, some items, which are necessary for the map, are not present in the topographic base. In this paper we deal with landcover themes, namely rocks, screes and glaciers, which are missing in the database and whose representation in mountainous area maps seems to be necessary. As the present maps are not very up to date for these themes, we did not want to simply extract this information from the existing paper maps. So we tried to design an automatic process to extract this information out of an orthophoto data base BDOrtho: this data base is made aside the topographic base, and consists of digital mosaicked colour orthophotos with a 50 cm resolution.

At first sight this could seem to be an easy problem. Lot of work has already been done for extracting landcover information from digital images (aerial or satellite) and, moreover, in our case we are only interested in a rather simple landcover legend. At second sight, this is not so easy for three reasons. First, in mountainous regions, the illumination effects are very important: about one fourth of the glaciers lie in the shade, so the precise determination of the shaded areas will be necessary. Secondly, the image data is a mosaic of scanned aerial photographs. The precise time of data capture is no more available, and the exact image processing is unknown, involving different interactive operations including different scalings, dodging, and even work with PhotoshopTM along the seams. Thirdly, we want a fully automatic procedure, which implies to design a sort of auto-learning adaptive method.

We will first present the proposed method for correcting the illumination effects. Then the interpretation scheme will be developed. In the last section, the experimental results will be presented.

2. CORRECTIONS FOR ILLUMINATION EFFECTS

The general model used has already been presented in (Le Men, H.1987; Boldo, D.2001) It implies the determination, for each pixel, of a mask of direct illumination, the computation of the visible sky solid angle and the estimation of the ground retro-illumination. The atmospheric model has a single parameter which is directly linked to ground visibility. It gives for each pixel the illumination (direct+diffuse) relative to flat open illumination. The second step will then be to correct this difference of illumination, which is not so easy as the radiometric transfer function for these images is unknown (and highly non-linear).

2.1 Determination of Shaded Areas

We will use an available digital terrain model (DTM) whose accuracy is about 10-20 m in altitude for these areas, with local errors over 50m. This is not sufficient for a precise computing of the shadows, especially as the errors are most important on the ridges (the DTM is too smooth). Even if a precise DTM were available, an uncertainty due to the acquisition time would remain. For managing this uncertainty, we will use the probability estimation of shadow knowing DTM, and of shadow knowing the image. The probability of shadow knowing DTM is computed for a given time of data capture with the following method. We assume a gaussian error for the DTM, and compute the probability that a given pixel is sun-illuminated. The probability that a point M0 (altitude z0) is not hidden by a point Mi (altitude zi), belonging to the plane containing M and the sun (with elevation S), at distance di from M is $\text{erf}(hi+z0-zi)$, where erf is the repartition function of the gaussian error of the DTM and $hi = di \cdot \text{tg}S$. Assuming an independent choice of points M (which in fact is the case in our algorithm; see section 2.2), the probability that M0 is in the shadow is

$$1 - \prod_i \text{erf}(hi + z0 - zi)$$

This is done each five minutes for the interval of plausible data capture time (beginning and end of the flight). We then retain the maximum probability over this interval (in fact this should be seen as a possibility measure).

Figure 1 shows this probability image, knowing DTM, for an extract 380 x 380 pixels of the full zone. All the following illustrations will be provided on this area.

The probability of shadow knowing image is simply a look up table on the image which is automatically computed with the assumption that the reflectance probability is not dependant on the illumination. It uses the radiometric correction model (equ. 4, below). With these hypothesis, $F(i)$ is the corrected radiometry for the radiometric count i in the shadow, H the probability of radiometric count i (histogram of the image), G the probability of corrected radiometric count i and p the total probability of shadow then the Bayes law gives:

$H(i) = p G(F^{-1}(i)) + (1-p) G(i)$. This equation is solved by histogram equalisation, with a regularity criterion on F (curvature minimisation).

Figure 2 shows the orthophoto (channel red) and figure 3 shows the probability of shadow, knowing the image.

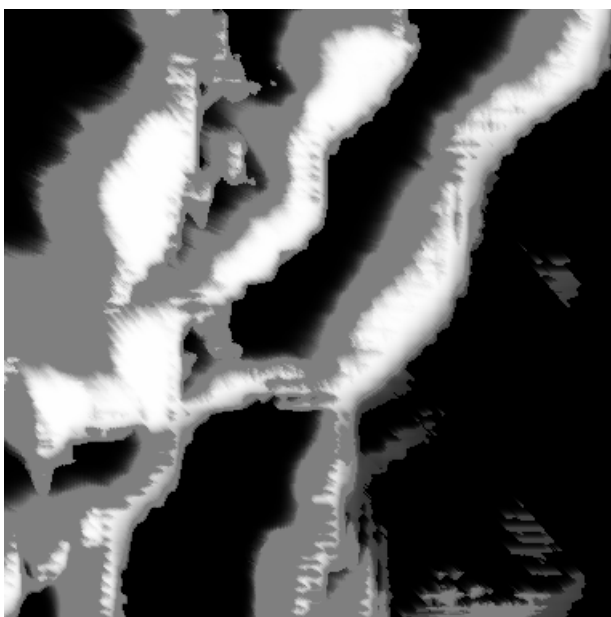


Figure 1. Probability of shadow knowing DTM

One can notice the low value of probability of shadow knowing the image on the glaciers in the shadow.

A data fusion using Dempster Shafer (Shafer, G. 1976, Dubois, D.1987) rule, will now give for each pixel a "probability" function for the shadow. In order to take into account the fact the shadows is not a local phenomenon but implies zones, we computed an image segmentation with a watershed algorithm using the gradient in the red channel (Guigues, L .2001). This gives a rather precise description in 110 000 regions and exact geometric localisation of the limits. The probability for zones is simply the mean probability of the pixels.

The final result is then obtained with a markovian model, implemented with a simulated annealing. Each region has a binary label: shadow or not shadow. The cost function is composed of two terms: neighbourhood cost as an exponential function of the mean radiometric difference along the border, and local function which is the function previously computed for each zone.

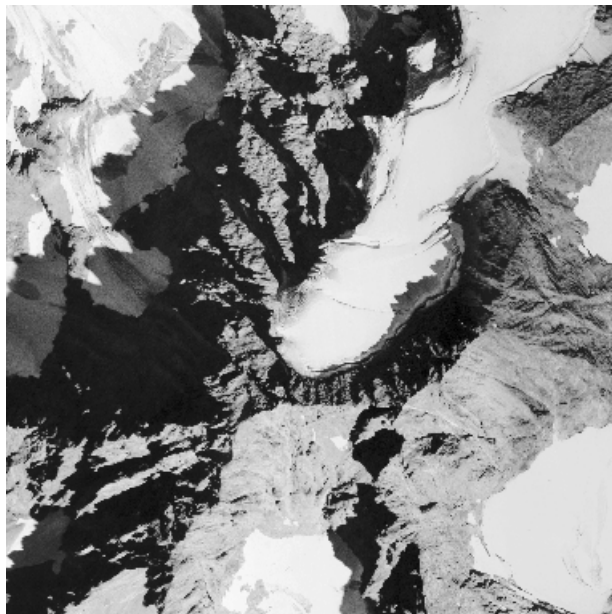


Figure 2. orthophoto- channel red

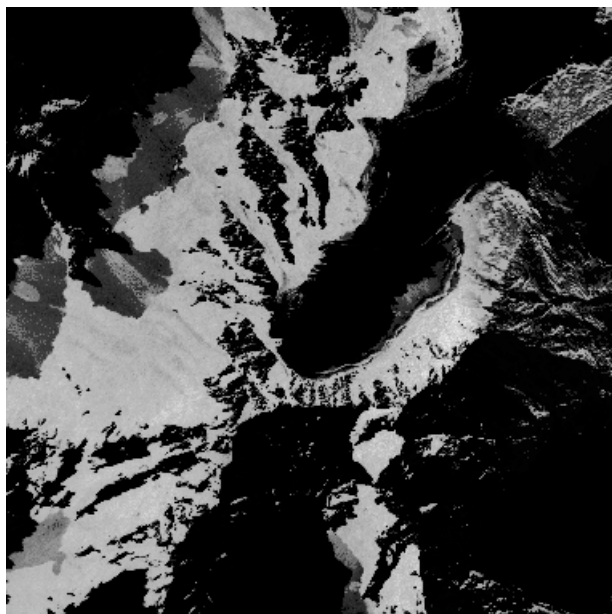


Figure 3. probability of shadow knowing image (channel red)



Figure 4. image mask of the shadows.

On the whole area the shadows represent 8.5% of the surface.

2.2 Diffuse Light

The second source of illumination is diffuse light with two sources: sky illumination and ground illumination.

For each pixel the solid angle of visible sky is computed. The directions are sampled with step $\pi/200$. For each direction, the point determining the visible sky is determined using the DTM. This can be done in a linear time, with the remark that on a given direction, for a given current point, its limiting point belongs to the list of the limiting points previously examined. The ground contribution is computed for each pixel, each direction with the integration of the image values for visible ground.

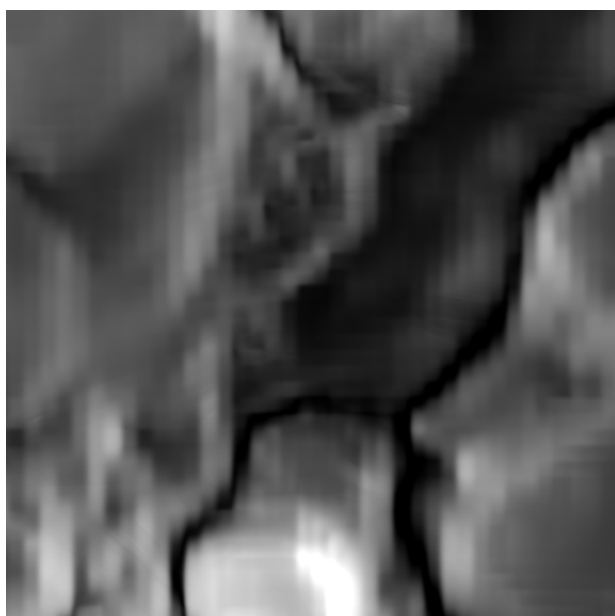


Figure 5. retro illumination from the ground.
Values vary between 0.005 and 0.2 on this extract.

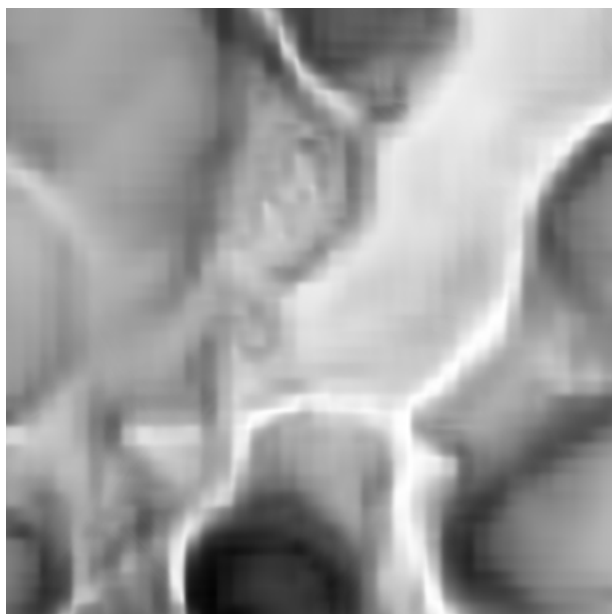


Figure 6. Sky illumination. Values vary between 0.6 and 1, on this extract

Though linear with the image size, this algorithm requires a lot of computing time (see sect.4), mainly due to the summation of the ground contribution from the image. This last term is very often negligible. But in the case of shaded areas with high slopes it can be the dominant term for the global illumination. This is why it cannot be neglected.

2.3 Total Illumination

The total illumination is the sum of these three terms with coefficients given by an atmospheric model (Le Men,H. 1987; Le Men,H. 1996). We must note here that we must take into account the variation of atmospheric diffusion with the altitude. This effect is important as the altitude varies in our test case from 500 to 3500m. Of course, in altitude the proportion of diffuse light is much smaller (in our model the height scale of the exponential density for aerosols is 1448 m in this domain) so that the shadows are much denser.

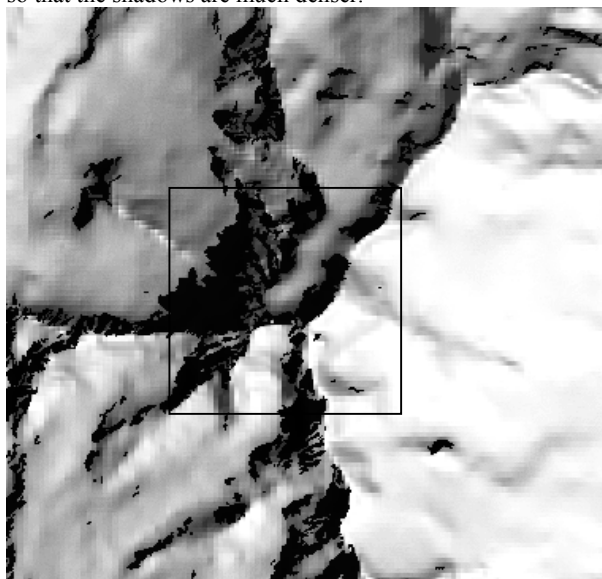


Figure 7. Total illumination

Values vary between 0.04 and 1.2. (1 is the value for an open flat ground). The histogram is strongly bimodal, showing a peak of shadowed areas around 0.06 and a second peak around 1 for flat open ground. The previous illustrations are smaller extracts on the centre of this image.

2.4 Radiometric Transfer Function Model

The digital count on the image is linked with the energy diffused by the ground through a transfer function F. If we note E the illumination, r the ground reflectance and I the image value:

$$I=F(E.r). \tag{1}$$

Correcting the image is replacing I with $I_c=F(E_0.r)$, where E_0 is a reference value for illumination on an open flat ground. From (1) we get

$$I_c=F(E_0 F^{-1}(I)/E) \tag{2}$$

The ratio E/E_0 is the illumination previously computed, E_c , so that:

$$I_c=F(F^{-1}(I)/E_c) \tag{3}$$

We will use for F the expression used in (Le Men,H.2000), which takes into account the logarithmic form of the density function for the negative film, the linear inversion of the scanner and a gamma applied during the analogue/digital conversion.

$$F=255 (1-(a r + b)^{-\gamma_1})^{\gamma_2} \tag{4}$$

$$I_c=255 \{1-[(1-I/255)^{1/\gamma_2} - 1/\gamma_1 - b]/E_c + b\}^{-\gamma_1} \gamma_2$$

Where b, γ_1 and γ_2 are parameters that are estimated so that the difference of cumulated histograms for shaded and non-shaded areas is minimised (hypothesis of independence between reflectance and illumination).

Though already complicated, this model does not lead to a perfect correction in the shadows. But, for the purpose of interpretation alone, the perfect correction is not necessary. As a matter of fact, since we know the information shadow/non shadow, separate interpretation for the two cases could be done.

This result is to be compared to figure 2 (original image). The dynamic of these two images is the same, since no correction is made on flat open ground. The correction is rather good in the glacier (the former limit of the shadow is hardly visible). In the rocky areas, the poor signal to noise ratio does not allow a good correction, with some parts over-corrected and some parts under-corrected. Nevertheless, the mean values are correct.

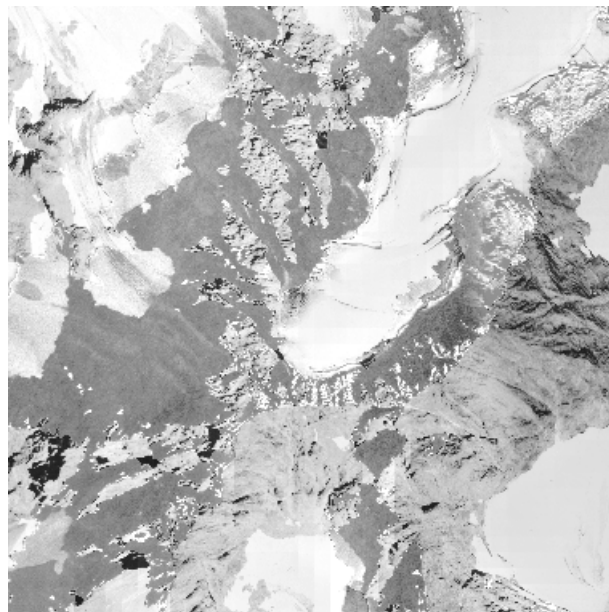


Figure 8. Result of the correction for illumination effects.

3. IMAGE INTERPRETATION

3.1 Prior Information

The image information is clearly insufficient for a correct discrimination of some themes. For example glaciers and riverbed rocks have very close digital counts (almost saturated white). Here also we will use prior information from the DTM: altitude, slope and orientation.

For each theme a prior probability given altitude (resp. slope, orientation) is estimated using known information (Elhai.,H.1968; Lacambre,A. 2001) For example we know that the upper limit for forest in the central alpine region is between 1800 and 2000m, depending on the orientation, that surface water can be found only in very flat areas, that glaciers cannot be found below 2300m, that the upper limit of vegetation is 3000m .

This information is formalised with piecewise linear functions, separately for altitude and slope. The orientation is taken into account only for forest and glacier (the other themes are roughly insensitive to orientation):

$$\Pr(\text{forest}/\text{altitude}=z, \text{azimuth}=az) = \Pr(\text{forest}/\text{altitude}=z+\text{slope}*\cos(az))$$

$$\Pr(\text{glacier}/\text{altitude}=z, \text{azimuth}=az) = \Pr(\text{glacier}/\text{altitude}=z-\text{slope}*\cos(az))$$

Where slope is expressed in %, limited to 200%.

The fusion of altitude, slope, orientation information is then obtained according to the following expression:

$$\Pr(\text{theme}/\text{DTM})= \frac{\Pr(\text{theme}/\text{altitude, orientation}) * \Pr(\text{theme}/\text{slope})}{\sum \Pr(\text{theme}/\text{altitude, orientation}) * \Pr(\text{theme}/\text{slope})}$$

This gives for each pixel a prior probability for each theme knowing the DTM.

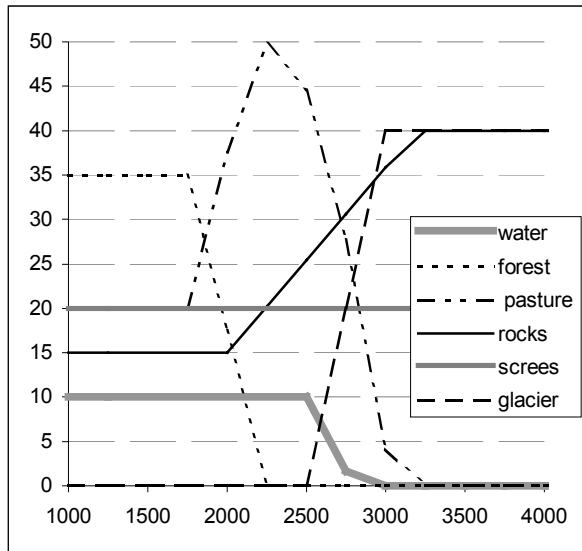


Figure 9. prior probability (in %) knowing altitude (in meter)

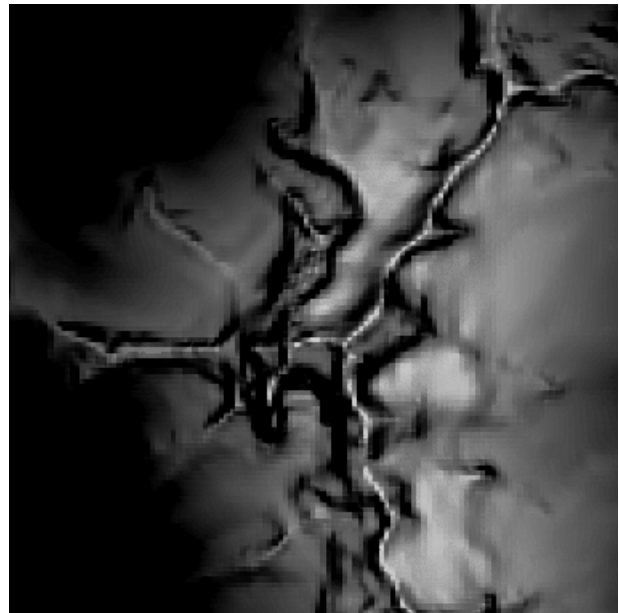


Figure 11. prior probability for glacier

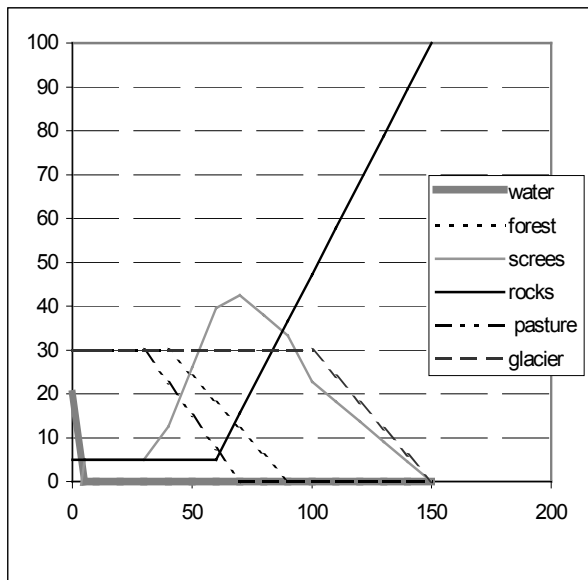


Figure 10. prior probability (in %) knowing slope (in %)

Figure 11 gives as an example the a priori image for glacier: one can easily recognise the main real locations of glaciers. In fact the high probability areas are actual glaciers or former glaciers sites. This confirms, if needed, the strong interdependence between landcover and relief.

The high probability values on the ridges are a systematic error of the DTM, which is too smooth. This gives very low values of the slope on the ridges, which in this altitude gives a high probability for glacier. This artefact does not propagate because it is incompatible with the other information sources.

3.2 Image Information

The image information used will be only the intensity and hue. As a matter of fact the saturation channel contains mainly artefacts: the limits between original photos.

The classification scheme is based on the bi-dimensionnal histogram intensity-hue, iteratively merging the connected regions of this histogram, which are most connected in the image. This hierarchical classification process is stopped either to a fixed value of the connectivity criteria, either to a number of classes. The interpretation of classes in terms of landcover items is then made comparing the classes to a fixed standard classification pattern (which only says that glaciers have high intensity, red, that forest are green low intensity...).

So for each pixel a "probability" of belonging to each theme, knowing the image is computed.

The two sources of information (from image and from DTM) are then merged using Dempster-Shafer rule.

3.3 Other Sources

Other sources of information, if available, can be used with the same scheme (e.g. small-scale databases, old maps...). In our case we also used information of BD Carto, which contains a landcover layer including glacier, dated 1989, with spatial accuracy about 50m.

Note that the possibility of using any source of information with different geometric and thematic accuracy gives the possibility of using this process in an updating context. In this case, the old information can be used as an imprecise information. We just need to qualify the uncertainty due to evolution (e.g. since glaciers evolve only by progression or regression, a simple extinction function on both sides of the borders of old glaciers can model the probability function).

Finally, we compute the mean probability for each zone of the segmentation (previously used §2.1).



Figure 12. final interpretation, glaciers in white, rocks in dark grey, screes in light grey.

3.4 Cartographic Expression.

In order to obtain only zones with cartographic meaning (i.e. large enough, we used a 250 pixel minimum size threshold), a local fusion of small zones is made. The final label given to each zone is simply the most probable theme.

The themes rocks and screes are selected using slope information. Rocks are selected where slope is over 100% and screes where slope is over 50%.

This leads to the cartographic result shown in figure14. (the final map will be in colour). Glaciers are here in light grey, screes are represented by dotted lines along the slope and rocks with a pouncing pattern where slope is over 100%. Mountain pasture are not represented..

Figure 13 is the map we would have had without the lancover information.

4. EXPERIMENTATION- RESULTS

4.1 Computing Time

The chosen test zone corresponds to half a regular sheet of Top25 regular French map in the region of St Christophe-en-Oisans in the Oisans massif. The area covers 336 km² (24 x 14 km²). The BDOrtho on this area was made from true colour photographs acquired on July 24th and 25th 1998 between 9h and 10h30. The image size is 48000x 24000 pixels of 50cm. It has been subsampled to get a 2.5m pixel, which corresponds, to 1/10 mm at the map scale of 1/25 000.

The processing time for computing the illumination on this area is 27h for each colour on a DEC Alpha 400Mhz.

It is from far the longer task. The other phases require less than 3 hours overall.

4.2 Evaluation

There are no clear errors when comparing to the original orthophoto. Moreover, large areas of forest which were independently restituted as non forest are well classified (misinterpretation of the human operator is due to shadow but the forest is present on the actual map and most presumably was not cleared). The precise evaluation cannot be done only with photo interpretation, since for example, it is very often difficult to distinguish between glaciers and moraine (screes), because the bottom of the glaciers is often covered with rock dust. Further evaluation will need ground checking during summer.

Comparison with actual map does not give evidence for errors.

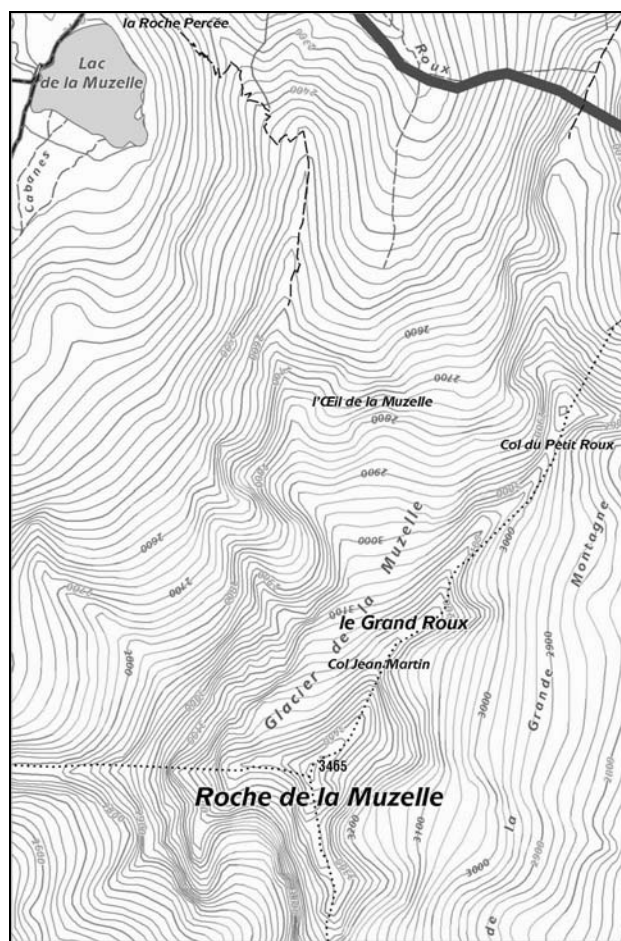


Figure 13. 1/25k map without the lancover themes

We have also checked with the topographic names database for presence of all named glaciers: all the named glaciers are detected.

Though this qualitative evaluation is encouraging, we will certainly find misclassification. The point here is that interactive correction is easy to implement and to use: since the image segmentation is geometrically accurate, interactive correction requires only one click, and we can already estimate that even a rate of 10% error could be interactively corrected in a few hours for one full sheet.

5. CONCLUSION

We presented a robust, fully automatic procedure for simple landcover image interpretation.

Apart from the algorithms for sky illumination and for the estimation of probability of shadow (§2.1) the whole process uses only well known image-processing techniques.

The main originality of this work, if any, is the bringing together of methods from different scientific backgrounds (mathematics, image processing, physics, and geography) with the systematic use of external data and knowledge and uncertainty management.

This last feature also allows the use of this approach in an updating context.

All this work has been done before the launch of SPOT5 using aerial photos resampled at 2.5m resolution. In the case of satellite images we could take advantage of a better radiometric homogeneity, leading to a better correction of the illumination effect. Moreover, the infrared channel will certainly give more information than the blue one for differentiation of landcover themes. On the other hand, difficulties could come from a higher viewing angle (hidden parts).

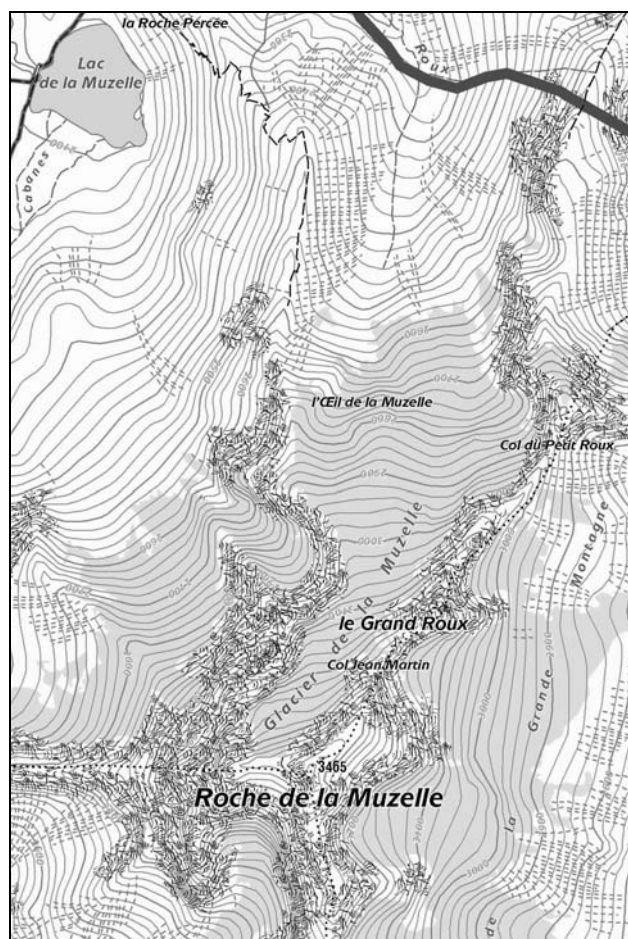


Figure 14. 1/25k map with the landcover themes extracted from the orthophoto

REFERENCES

- Boldo, D.- Le Men, H. 2001. Remote sensing model adaptation to very high resolution digital images of urban areas. *1st IEEE/ISPRS Joint Workshop on remote sensing and data fusion over urban areas*. Roma
- Dubois, D.- Prade, H. 1987. *Théorie des possibilités application à la représentation des connaissances en informatique* Masson
- Elhaï., H.1968. *Biogéographie*. Armand Colin. Paris
- Guigues, L.- Le Men, H.- Cocquerez, J.P.2001. Segmentation d'image par minimisation d'un critère MDL dans une pyramide de segmentations. In *Actes du congrès GRETSI Signal and Image Processing*, Toulouse, France,
- Lacambre, A. 2001. Aléas et risques naturels en milieu montagnard; apport et limites d'un système d'information géographique. Thèse de l'Université Paris 4.
- Le Men, H. 1987. Etude de la stéréoradiométrie sur les images Spot. Colloque Spot1. CNES Paris Cepadues.ed.
- Le Men, H. 1996. Mémoire d'habilitation à diriger les recherches Université Paris 5
- Le Men, H. -Boldo, D.2000. *Mosaïque automatique d'orthophotographies*. RFIA . Paris
- Shafer, G. 1976. *A mathematical theory of evidence* Princeton university press .

